

Article

Glyco-Nanovesicles with Activatable Near-Infrared Probes for Real-Time Monitoring of Drug Release and Targeted Delivery

Shoupeng Cao, Zhichao Pei, Yongqian Xu, and Yuxin Pei

Chem. Mater., **Just Accepted Manuscript** • DOI: 10.1021/acs.chemmater.6b01857 • Publication Date (Web): 31 May 2016

Downloaded from <http://pubs.acs.org> on June 6, 2016

Just Accepted

“Just Accepted” manuscripts have been peer-reviewed and accepted for publication. They are posted online prior to technical editing, formatting for publication and author proofing. The American Chemical Society provides “Just Accepted” as a free service to the research community to expedite the dissemination of scientific material as soon as possible after acceptance. “Just Accepted” manuscripts appear in full in PDF format accompanied by an HTML abstract. “Just Accepted” manuscripts have been fully peer reviewed, but should not be considered the official version of record. They are accessible to all readers and citable by the Digital Object Identifier (DOI®). “Just Accepted” is an optional service offered to authors. Therefore, the “Just Accepted” Web site may not include all articles that will be published in the journal. After a manuscript is technically edited and formatted, it will be removed from the “Just Accepted” Web site and published as an ASAP article. Note that technical editing may introduce minor changes to the manuscript text and/or graphics which could affect content, and all legal disclaimers and ethical guidelines that apply to the journal pertain. ACS cannot be held responsible for errors or consequences arising from the use of information contained in these “Just Accepted” manuscripts.

Glyco-Nanovesicles with Activatable Near-Infrared Probes for Real-Time Monitoring of Drug Release and Targeted Delivery

Shoupeng Cao, Zhichao Pei, Yongqian Xu, and Yuxin Pei*

Shaanxi Key Laboratory of Natural Products & Chemical Biology, College of Science, Northwest A&F University, Xinong Road 22, Yangling, Shaanxi 712100 (P.R. China)

ABSTRACT: A glyco-nanovesicle (Lac-SS-DCM) is self-assembled by a rationally designed amphiphilic lactose derivative (**1**), which features a surface lactose corona, disulfide linkage, and an activatable DCM NIR probe moiety. Taking advantage of the disulfide linkage, Lac-SS-DCM can be triggered to disassemble by glutathione (GSH) and simultaneously activate the dormant NIR, which allows for a drug-loaded vesicle capable of both therapies in cancer cells where higher GSH concentration exists and real-time monitoring of drug release. Furthermore, Lac-SS-DCM demonstrates excellent HepG2 target ability as well as higher anticancer efficacy and reduced side effects compared to free DOX through lactose-mediated endocytosis resulting from the surface lactose corona, which acts as multivalent galectin-targeting ligands. As a multifunctional drug delivery with perfect synchronization of targeting, imaging, monitoring, and controllable drug release, we believe this activatable glyco-nanovesicle, readily modulated for imaging of different tumors by incorporation of unique targeting entities on the vesicle surface, would be of broad interest for cancer diagnosis and therapy.

INTRODUCTION

Tracking of drug release in real time is of great importance in cancer chemotherapy,^{1,3} and particularly challenging owing to the limited modifying strategies for both drugs and dyes.^{4,5} For this purpose, a cancer-targeting theranostic prodrug, where gemcitabine was linked via a disulfide bond to coumarin moiety which was coupled with biotin as a targeting ligand, was developed.⁶ Considering that some essential antitumor drugs are non- or weakly fluorescent, and the difficulty in modifying each individual drug and/or dye,^{6,7} a multifunctional drug delivery system (MDDS) carrying activatable near-infrared (NIR) fluorescence dyes,⁸⁻¹¹ which allows for both real-time monitoring of drug release and targeted cancer therapy in response to a tumor-related stimulus,¹²⁻²⁰ is highly desired. Up to now, very few MDDSs carrying near-infrared (NIR) fluorescence dyes have been reported.²¹ Furthermore, they have mainly been constructed with amphiphilic macromolecules.²²

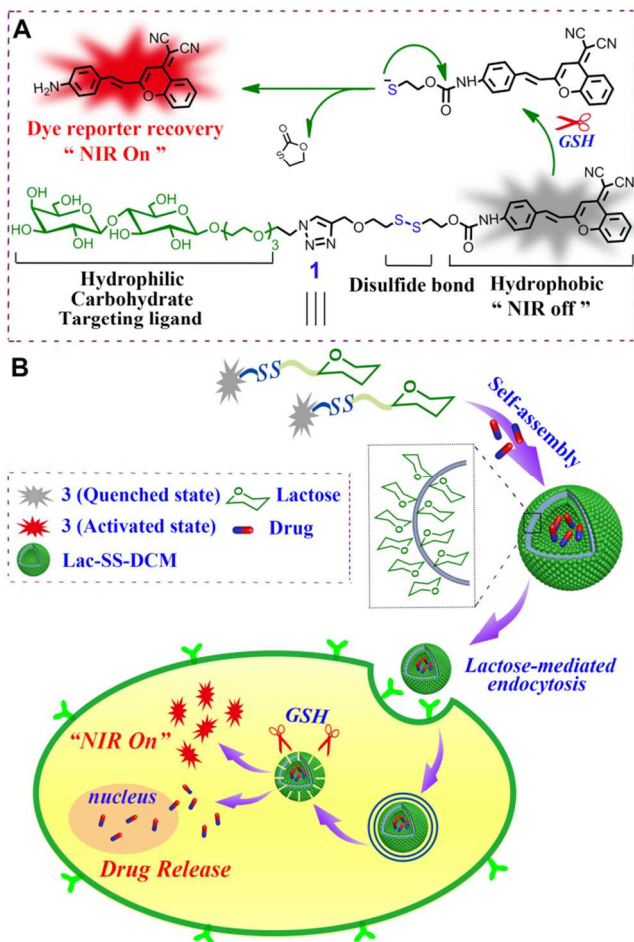
Compared with macromolecular counterparts, nanovesicles obtained via self-assembly of amphiphilic small molecules hold a significant advantage in the ability to be modified to obtain a wide range of desired functions via the incorporation of hydrophobic/hydrophilic components through rational selection.²³⁻³⁰ NIR fluorescence dyes with emission in the range of 650-900 nm are especially desirable for imaging in vivo due to their ability to penetrate tissue non-invasively with low background interference.^{31,32} Naturally, using a NIR dye as the hydrophobic component of a MDDS would be ideal,¹⁰ since most known NIR dyes, such as porphyrin and dicy-

anomethylene-4H-pyran (DCM) derivatives,^{10,33,34} are hydrophobic. In this work, a DCM dye was chosen due to their controllable emission wavelength, large Stokes shift, and high photostability for our MDDS.³⁴

Conversely, carbohydrates are outstanding hydrophilic building blocks with excellent biocompatibility.³⁵ Much attention have been placed on their potential as tumor cell targeting ligands based on the fact that malignant transformation of cells is often concomitant with overexpression of specific glycoproteins (lectins) on the cell surfaces.³⁶ Thus, glyco-nanovesicles formed by carbohydrate derivatives will have great potential as MDDS for tumor targeting via carbohydrate-lectin specific interactions.³⁷⁻³⁹ To the best of our knowledge, there have been no reports of glyco-nanovesicles carrying activatable near-infrared probes for both real-time monitoring of drug release and targeted delivery.

Thus, an amphiphilic compound **1**, in which a DCM moiety (as the hydrophobic part and the fluorescence off-on probe), pre-quenched and conjugated with a lactose derivative (as the hydrophilic part and the targeting ligand) via a disulfide linkage (the GSH-responsive unit), was synthesized and self-assembled to lactose-capped supramolecular glyco-nanovesicles (Lac-SS-DCM) in aqueous solution (Scheme 1). The Lac-SS-DCM was evaluated for the potential of real-time NIR monitoring of drug release and targeted cancer therapy, where the lactose corona on the surface of the vesicle can act as multivalent targeting ligands to galectin overexpressed on HepG2 cells,³⁶ via enhanced carbohydrate-protein interactions

Scheme 1. Schematic illustration of assembly, lactose-mediated endocytosis, NIR fluorescence on and drug release of Lac-SS-DCM.

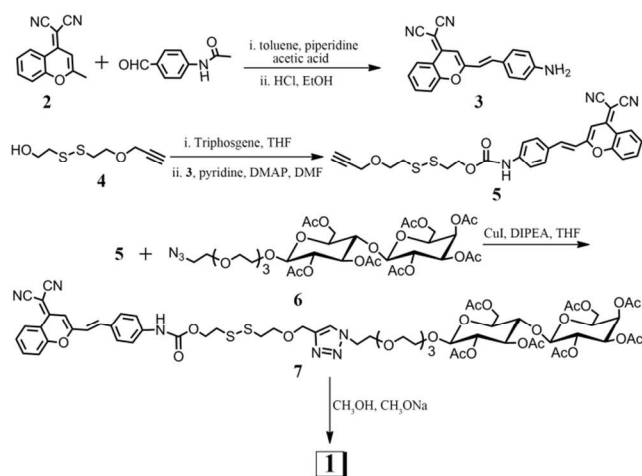


due to the “cluster effect”.^{35,40} To the best of our knowledge, this work represents the first MDDS based on glycol-nanovesicles, where key features of targeting, stimuli-response, therapy, and real-time NIR fluorescence monitoring are combined.

RESULTS AND DISCUSSION

The synthesis of **1** was performed by following the synthetic route outlined in Scheme 2. Compound **2** – **4** were prepared by adapting previously reported procedures.^{41,42} Compound **5**, a DCM derivative featured with a disulfide bond unit and an alkyne reaction group, is a key intermediate and was synthesized with 67 % yield from compound **3** and **4** in a one-pot procedure,^{41–44} where the strong NIR fluorescence light of compound **3** was quenched by the newly formed amide bond. Thereafter, **5** clicked with compound **6** (a lactose azide derivative) via CuAAC reaction to give compound **7** in 66 % yield.^{45–47} The deprotection of **7** by sodium methanol resulted in the target compound **1** with 96 % yield.⁴⁵ The chemical structures of **5**, **7**, and **1** were confirmed by ¹H NMR, ¹³C NMR, and HRMS analyses, respectively. The synthetic details and characterization of **1** – **7** can be found in the Supporting Information (SI).

Scheme 2. The synthetic route of Compound 1



The self-assembly of compound **1** in water was then investigated. By subjecting an aqueous solution of **1** to sonication for 20 min, a clear Tyndall effect was observed (Figure 1a, left). This clearly indicated the existence of abundant nanospecies. Further characterization with scanning electron microscopy (SEM, Figure 1b) and transmission electron microscopy (TEM, Figure 1c) proved the nanospecies were spherical vesicles with a wall thickness of 2.8 nm. The analysis with dynamic light scattering (DLS, Figure 1d) showed that the average diameter and polydispersity index of Lac-SS-DCM were 232 nm and 0.267, respectively. The critical aggregation concentration (CAC) of **1** in water was calculated to be 34 μ M by plotting the surface tension of the solution as a function of the concentration (Figure S16).

Upon the addition of glutathione (GSH, 2 mM), distinct Tyndall effect observed previously with Lac-SS-DCM disappeared, accompanied with the formation of a brown precipitate at the bottom of the quartz cuvette (Figure 1a, right). DLS analysis showed that the nanovesicles transformed to aggregates with an average diameter in the

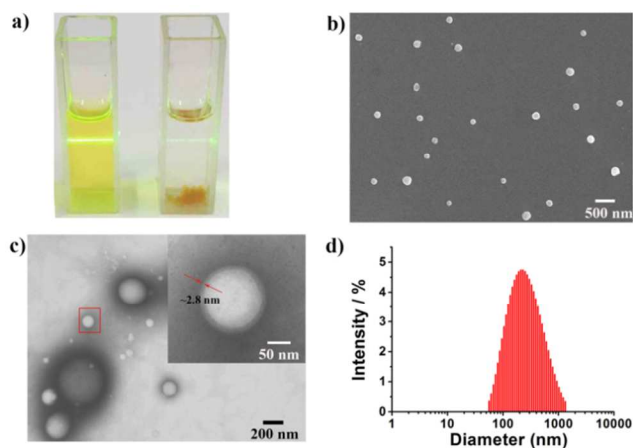


Figure 1. a) Tyndall effect of Lac-SS-DCM (left) and precipitates formed in the redox environment (right); b) SEM image of Lac-SS-DCM; c) TEM image of Lac-SS-DCM. Inset: Enlargement of the image marked in the red frame; d) DLS analysis of Lac-SS-DCM.

micron scale (Figure S15a). These results implied the disassembly of Lac-SS-DCM due to the decomposition of **1** caused by the reduction of the disulfide bond by GSH.

Next, the NIR fluorescence restoration of the quenched DCM probe **1** was investigated with a UV-Visible spectrophotometer. **1** displayed a typical ICT broad absorption band centered at 450 nm and a relatively weak emission at 560 nm in PBS/DMSO buffer solution (50/50, v/v, pH = 7.4, 10 mM, Figure 2). Upon the addition of GSH (2.0 mM), the absorption peak red shifted to 490 nm, accompanied by a rapid color change from bright yellow to orange under daylight (and dark to bright red under UV lamp, Figure S10). Meanwhile, a strong NIR fluorescence emission peak at 650 nm with ~34-fold enhanced intensity and a large Stokes shift of 160 nm were observed, which are highly desirable for high quality optical monitoring and imaging in vivo.

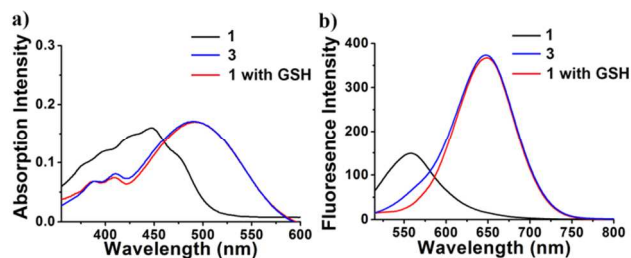


Figure 2. Absorption (a) and emission (b) spectra of compound **3** (blue), and **1** in DMSO/PBS solution (50/50, v/v, pH = 7.4, 10 mM) at 37 °C in the absence (black) and presence (red) of GSH for 1 h. Concentration for **1** and **3**: 10.0 μ M, GSH: 2 mM; λ_{ex} = 490 nm.

More importantly, the overlaps of the absorption and fluorescence spectra of **1** after treatment with GSH to those of **3** clearly indicated that **3** was successfully released as anticipated via cleavage of the disulfide bond by reacting with GSH, and the subsequent intramolecular cyclization.³⁴ This was further confirmed with electrospray ionization mass spectrometry, where both peaks of 312.54 (corresponding to [**3** + H⁺]) and 104.96 (corresponding to [1,3-Oxathiolan-2-one + H⁺], a byproduct from the intramolecular cyclization), were found from the resultant mixture of **1** with GSH (Figure S17). Further studies on the fluorescence recovery of Lac-SS-DCM indicated that Lac-SS-DCM possesses fast and specific response to GSH in biological environments (Figure S11, S12), and can act as a direct off-on signal reporter for drug release.

The GSH-responsive property of Lac-SS-DCM was further studied with HepG2 (a hepatoma carcinoma cell) living cells by confocal laser scanning microscopy (CLSM) and flow cytometry. As shown in Figure 3a-d, red fluorescence in the cytoplasm of HepG2 cells was observed clearly after 4 h of incubation with 10 μ M of Lac-SS-DCM. In contrast, an obvious fluorescence enhancement was seen under the same conditions except the addition of GSH (2.5 mM) to the culture medium (Figure 3e-h), which was attributed to the accelerated cleavage of disulfide bond

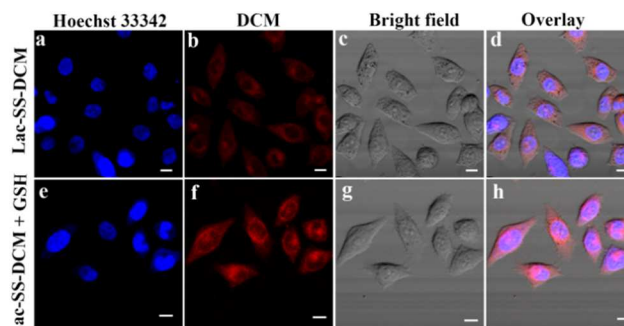


Figure 3. CLSM images of HepG2 cells cultured with Lac-SS-DCM (10 μ M) in the absence (a-d) or presence (e-h) of extra 2.5 mM GSH for 1 h. Nucleus was stained with Hoechst 33342. Images were taken from the Hoechst 33342 channel (a and e), DCM channel (b and f), bright field (c and g), and overlay (d and h). Scale bar is 10 μ m.

resulting from a higher intracellular GSH concentration. Flow cytometry analysis for HepG2 cells incubated with Lac-SS-DCM in the absence or presence of GSH in the culture medium for different time periods and disclosed similar results (Figure S18). Hence we conclude that Lac-SS-DCM possesses satisfying GSH-responsive property, which is important for targeted cancer therapy.

A lactose corona, which is formed on the surfaces of Lac-SS-DCM due to the lactose moiety in **1**, is expected to endow the vesicles galectin recognition ability. To evaluate the target recognition ability of Lac-SS-DCM, normal (293T) and cancer (HepG2 and HeLa) cells were incubated with Lac-SS-DCM at 10 μ M for 4 h, respectively. The

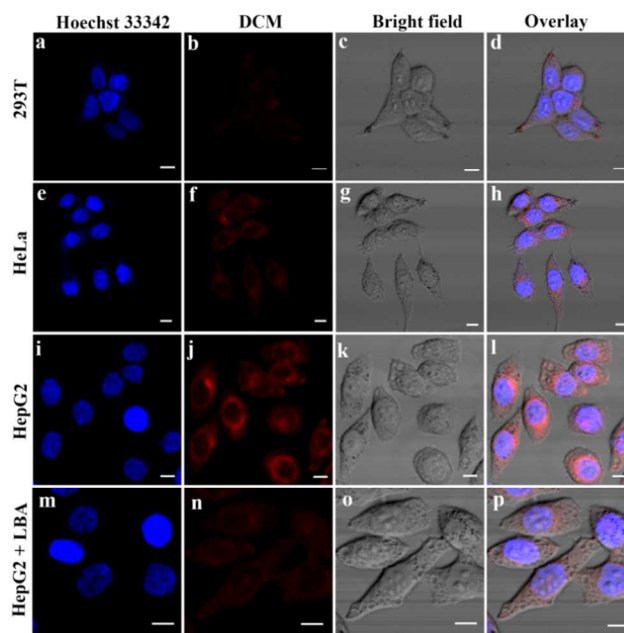


Figure 4. CLSM images of 293T (a-d), HeLa (e-h) and HepG2 (i-l) cells cultured with Lac-SS-DCM (10 μ M) for 4 h. Confocal laser scanning microscopy images (m-p) HepG2 cultured with Lac-SS-DCM for 4 h pre-incubated with LBA for 4 h. Nucleus was stained with Hoechst 33342. Images were taken from the Hoechst 33342 channel (a, e, i and m), DCM channel (b, f, j and n), bright field (c, g, k and o), and the overlapped image (d, h, l and p). Scale bar is 10 μ m.

cellular uptake and the intensity of NIR fluorescence were investigated with CLSM. As shown in Figure 4, strong fluorescence was observed in the cytoplasm of HepG2 cells (Figure 4i-l), which are known to overexpress galectins on their cell membrane; whereas rather low or negligible fluorescence was seen with HeLa (Figure 4e-h) and 293T cells (Figure 4a-d) under the same conditions. In addition, HepG2 cells pre-incubated with lactobionic acid (LBA, 2 mg/mL) for 4 h were incubated with Lac-SS-DCM for comparison. Pre-incubation of HepG2 cells with LBA led to a dramatic decrease in fluorescence (Figure 4m-p), which was further confirmed by flow cytometry (Figure S19). The decrease in fluorescence indicated that Lac-SS-DCM targets hepatoma through endocytosis via lactose-mediated active process, and the presence of LBA led to the blockade of lactose receptor, which subsequently inhibited lactose-mediated endocytosis; cellular uptake was thus only driven by non-specific endocytosis as with HeLa and 293T cells.

In addition, cell viability studies by methyl thiazole tetrazolium (MTT) cell survival assay disclosed that the cytotoxicity of Lac-SS-DCM is negligible even with prolonged incubation (72 h) under a high concentration (Figure S21). All the results mentioned above suggest that Lac-SS-DCM may be applied for hepatoma-targeted recognition and imaging. Although there are concerns regarding that the selectivity of lactose *in vivo* to hepatoma cells might be compromised owing to that galectins express on the membrane of healthy liver cells,⁴⁸ strong hepatoma-targeting property of lactose at both cellular and animal levels^{49,50} indicates Lac-SS-DCM has the potential for preferential accumulation in tumors.

The drug loading of Lac-SS-DCM was studied using doxorubicin hydrochloride (DOX), a typical hydrophilic anticancer drug as a model. Upon the loading of DOX into Lac-SS-DCM, the solution, similar to that of Lac-SS-DCM, showed clear Tyndall effect, apart from a color change from yellow to brown (Figure 5a, inset). DLS analysis showed the average diameter of DOX-loaded Lac-SS-DCMs to be 360 nm, which is larger than that of the unloaded vesicles. This coincides roughly with the result obtained by SEM, which showed that the average diameter of the DOX-loaded vesicles to be 300 nm (Figure 5b). The loading of DOX into Lac-SS-DCM was further confirmed by UV-Vis spectrum of DOX-loaded vesicular solution, where a new absorption band at the range of 400–520 nm, which corresponds to DOX, was observed (Figure 5c). The encapsulation efficiency of DOX was calculated to be 32 wt. % by UV-Vis spectroscopy, which indicated a good drug-loading capability.

To study the release profile of Lac-SS-DCM, fluorescein sodium (NaFL), a hydrophilic fluorescent dye giving green emission, was used instead of DOX to avoid fluorescence overlap with **3** (Figure S13). As shown in Figure 5d, the amount of NaFL released by NaFL-loaded Lac-SS-DCM was 22 %, 32 %, and 73 % of encapsulated NaFL in PBS

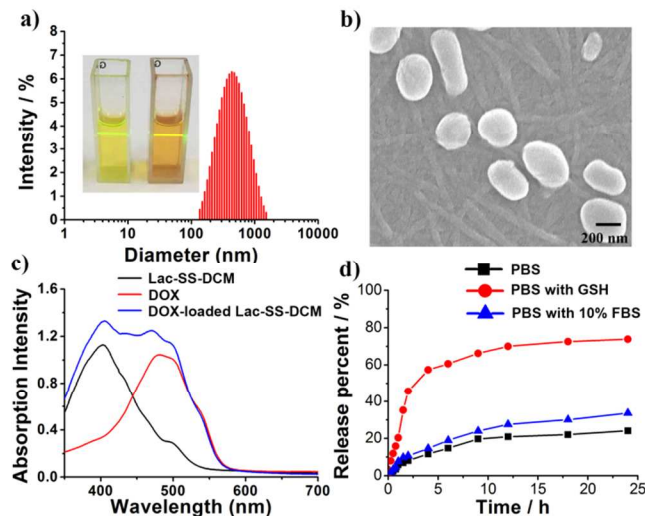


Figure 5. a) DLS analysis of DOX loaded Lac-SS-DCM. Inset: Tyndall effect of Lac-SS-DCM (left) and DOX-loaded Lac-SS-DCM (right). b) SEM image of the DOX-loaded Lac-SS-DCM. c) UV-Vis absorption of Lac-SS-DCM, free DOX and DOX-loaded Lac-SS-DCM. d) Release profiles of NaFL-loaded Lac-SS-DCM in PBS, PBS with FBS (10 %), or PBS with GSH (2 mM), respectively. In all the cases, pH was 7.4.

(pH 7.4), PBS with FBS (10 %), or PBS with GSH (2 mM) within 24 h, respectively. In addition, clear Tyndall effect of Lac-SS-DCM solution with 10 % FBS in PBS was observed after 48 h (Figure S14). These results suggest that NaFL-loaded Lac-SS-DCM are fairly stable under physiological condition and can be used for controllable release.

If an antitumor drug is non- or weak fluorescent, tracking of the drug *in vitro* or *in vivo* is particularly challenging owing to the limited modifying strategies for both drugs and dyes. However, with Lac-SS-DCM, the recovery of NIR dye of **3**, resulted from the cleavage of disulfide bond when exposed to GSH, happens simultaneously with the disassembly of the vesicles and the release of the encapsulated payload. Thus, the information on where and when the drug was released along with the distribution can be conveniently obtained by fluorescence imaging. To illustrate the ability of intracellular monitoring and fluorescence recovery of Lac-SS-DCM, a co-localization experiment was performed, where HepG2 cells were incubated with 10 μ M NaFL-loaded Lac-SS-DCM for 0.5, 1, 2, and 4 h, respectively. The fluorescence images of the cells were taken by CLSM (Figure 6). Merging of green fluorescence emitted by NaFL ($\lambda_{em} = 512$ nm) and NIR fluorescence signal emitted by **3** ($\lambda_{em} = 650$ nm) demonstrated co-localization as indicated by the yellow areas. Furthermore, flow cytometry analysis for HepG2 cells incubated with NaFL-Loaded Lac-SS-DCM for different time periods disclosed similar results mentioned above (Figure S20). The results proved the feasibility of real-time monitoring of the drug release process with Lac-SS-DCM *in vitro*.

To evaluate the anticancer efficiency of DOX-loaded vesicles, 293T, HeLa, and HepG2 cells were incubated with DOX-loaded vesicles and free DOX for 24, 48, and 72

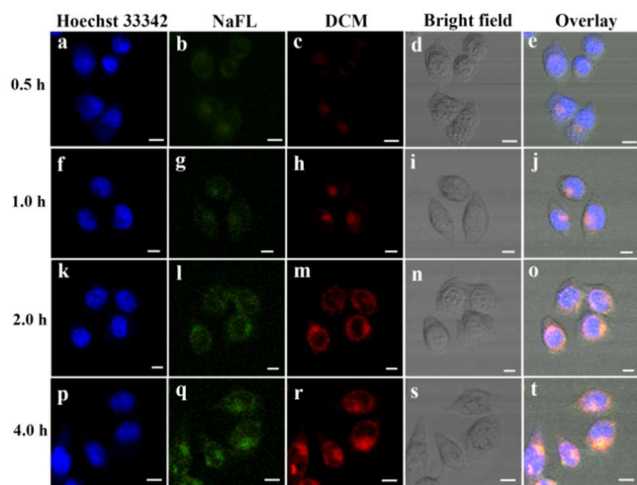


Figure 6. CLSM images of HepG2 cells cultured with NaFL-loaded Lac-SS-DCM (10 μ M) for 0.5, 1, 2, and 4 h, respectively. Images were taken from the Hoechst 33342 channel (a, f, k, and p), NaFL channel (b, g, l, and q), DCM channel (c, h, m, and r), bright field (d, i, n, and s), and overlay (e, j, o, and t), respectively. Scale bar is 10 μ m.

h, respectively. As can be seen in Figure 7, the relative viabilities of 293T cells after incubation with DOX-loaded vesicles (2.0 μ M corresponding to DOX) at all three tested time periods were visibly higher than those with free DOX. In contrast, HepG2 cells under the same conditions showed lower relative viabilities after incubation with DOX-loaded vesicles than with free DOX. Meanwhile, HeLa cells under same condition show similar result compared with 293T cells (Figure S22). These results indicated that the encapsulation of DOX with Lac-SS-DCM could enhance the drug efficacy against HepG2 hepatoma cells while reducing its cytotoxicity to normal cells. This result further confirmed the purpose of our rational design to obtain hepatoma cell targeting Lac-SS-DCM via the enhanced specific interaction between lactose-corona on the surface of Lac-SS-DCM and the galectin overexpressed on HepG2 cell surface through the “cluster effect”. All these results indicated that Lac-SS-DCM is an excellent biocompatible MDDS, and can be used for both real-time NIR monitoring of drug release and targeted cancer therapy.

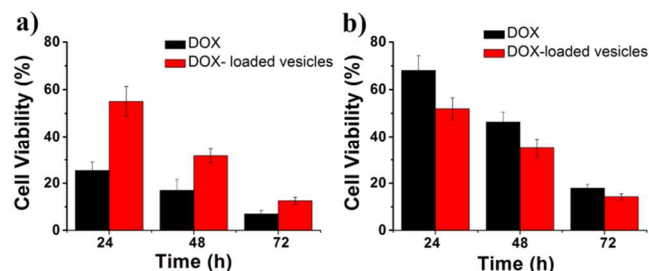


Figure 7. Comparison of DOX and DOX-loaded vesicles on viabilities of 293T cells (a) and HepG2 cells (b) for 24, 48, and 72 h, respectively. Concentration of DOX: 2.0 μ M.

CONCLUSIONS

In summary, we have successfully developed a glyco-nanovesicle of Lac-SS-DCM, which is self-assembled by a rationally designed amphiphilic lactose derivative (**1**) that is composed of a DCM moiety as a NIR fluorescent reporter, a disulfide bond as a GSH-responsive cleavable linker, and a lactose moiety as a hepatoma-targeting ligand. Lac-SS-DCM displays negligible cytotoxicity and good hepatoma-targeting ability due to the enhanced lactose-mediated endocytosis resulting from the lactose corona on its surface. DOX-loaded Lac-SS-DCM shows enhanced bioavailability and anticancer efficacy specifically to HepG2 cells with reduced side effect compared to free DOX. Most importantly, the cleavage of the disulfide bond in **1** caused by the high intracellular concentration of GSH leads to the activation of DCM fluorescence probe, disassembly of Lac-SS-DCM, and anticancer drug release all simultaneously, enabling real-time NIR monitoring of drug release, non-invasive cellular imaging, and targeted cancer therapy. Thus, Lac-SS-DCM, which is readily modulated for imaging of different tumors by incorporation of any individual targeting entity on the vesicle surface, would be of broad interests for cancer diagnosis and therapy.

ASSOCIATED CONTENT

Supporting Information

Supporting Information. Experimental procedures, characterizations, supplementary spectra and figures.

AUTHOR INFORMATION

Corresponding Author

*E-mail: peiyx@nwfufu.edu.cn

Notes

The authors declare no competing financial interests.

ACKNOWLEDGMENT

This research work was supported by the National Natural Science Foundation of China (NSFC 21572181 and 31270861) and Project of Science and Technology of Social Development in Shaanxi Province (2016SF-029).

REFERENCES

- (1) Kendall, M.; Lynch, I., Long-term monitoring for nanomedicine implants and drugs. *Nat. Nano.* **2016**, *11*, 206-210.
- (2) Kulkarni, A.; Rao, P.; Natarajan, S.; Goldman, A.; Sabbiseti, V. S.; Khater, Y.; Korimerla, N.; Chandrasekar, V.; Mashelkar, R. A.; Sengupta, S., Reporter nanoparticle that monitors its anticancer efficacy in real time. *Proc. Natl. Acad. Sci. U.S.A.* **2016**, *113*, E2104-E2113.
- (3) Chen, G.; Roy, I.; Yang, C.; Prasad, P. N., Nanochemistry and Nanomedicine for Nanoparticle-based Diagnostics and Therapy. *Chem. Rev.* **2016**, *116*, 2826-2885.
- (4) Lee, M. H.; Yang, Z.; Lim, C. W.; Lee, Y. H.; Dongbang, S.; Kang, C.; Kim, J. S., Disulfide-Cleavage-Triggered Chemosensors and Their Biological Applications. *Chem. Rev.* **2013**, *113*, 5071-5109.

- (5) Lim, E.-K.; Kim, T.; Paik, S.; Haam, S.; Huh, Y.-M.; Lee, K., Nanomaterials for Theranostics: Recent Advances and Future Challenges. *Chem. Rev.* **2015**, *115*, 327-394.
- (6) Maiti, S.; Park, N.; Han, J. H.; Jeon, H. M.; Lee, J. H.; Bhuniya, S.; Kang, C.; Kim, J. S., Gemcitabine-Coumarin-Biotin Conjugates: A Target Specific Theranostic Anticancer Prodrug. *J. Am. Chem. Soc.* **2013**, *135*, 4567-4572.
- (7) Zhu, L.; Wang, T.; Perche, F.; Taigind, A.; Torchilin, V. P., Enhanced anticancer activity of nanopreparation containing an MMP2-sensitive PEG-drug conjugate and cell-penetrating moiety. *Proc. Natl. Acad. Sci. U.S.A.* **2013**, *110*, 17047-17052.
- (8) Peer, D.; Karp, J. M.; Hong, S.; Farokhzad, O. C.; Margalit, R.; Langer, R., Nanocarriers as an emerging platform for cancer therapy. *Nat. Nano.* **2007**, *2*, 751-760.
- (9) Allen, T. M.; Cullis, P. R., Drug delivery systems: Entering the mainstream. *Science* **2004**, *303*, 1818-1822.
- (10) Li, Y.; Lin, T.-y.; Luo, Y.; Liu, Q.; Xiao, W.; Guo, W.; Lac, D.; Zhang, H.; Feng, C.; Wachsmann-Hogiu, S.; Walton, J. H.; Cherry, S. R.; Rowland, D. J.; Kukis, D.; Pan, C.; Lam, K. S., A smart and versatile theranostic nanomedicine platform based on nanoporphyrin. *Nat. Commun.* **2014**, *5*, 4712.
- (11) Taratula, O.; Doddapaneni, B. S.; Schumann, C.; Li, X.; Bracha, S.; Milovancev, M.; Alani, A. W. G.; Taratula, O., Naphthalocyanine-Based Biodegradable Polymeric Nanoparticles for Image-Guided Combinatorial Phototherapy. *Chem. Mater.* **2015**, *27*, 6155-6165.
- (12) Ferrari, M., Cancer nanotechnology: opportunities and challenges. *Nat. Rev. Cancer* **2005**, *5*, 161-171.
- (13) Mura, S.; Nicolas, J.; Couvreur, P., Stimuli-responsive nanocarriers for drug delivery. *Nat. Mater.* **2013**, *12*, 991-1003.
- (14) Li, C., A targeted approach to cancer imaging and therapy. *Nat. Mater.* **2014**, *13*, 110-115.
- (15) Torchilin, V. P., Multifunctional, stimuli-sensitive nanoparticulate systems for drug delivery. *Nat. Rev. Drug Discov.* **2014**, *13*, 813-827.
- (16) Liu, Q.; Jin, C.; Wang, Y.; Fang, X.; Zhang, X.; Chen, Z.; Tan, W., Aptamer-conjugated nanomaterials for specific cancer cell recognition and targeted cancer therapy. *NPG Asia Mater.* **2014**, *6*, e95.
- (17) Zhao, Z.; Meng, H.; Wang, N.; Donovan, M. J.; Fu, T.; You, M.; Chen, Z.; Zhang, X.; Tan, W., A Controlled-Release Nanocarrier with Extracellular pH Value Driven Tumor Targeting and Translocation for Drug Delivery. *Angew. Chem. Int. Ed.* **2013**, *52*, 7487-7491.
- (18) Guo, X.; Shi, C.; Yang, G.; Wang, J.; Cai, Z.; Zhou, S., Dual-Responsive Polymer Micelles for Target-Cell-Specific Anticancer Drug Delivery. *Chem. Mater.* **2014**, *26*, 4405-4418.
- (19) Yan, Y.; Such, G. K.; Johnston, A. P. R.; Best, J. P.; Caruso, F., Engineering Particles for Therapeutic Delivery: Prospects and Challenges. *ACS Nano* **2012**, *6*, 3663-3669.
- (20) Caruso, F.; Hyeon, T.; Rotello, V. M., Nanomedicine. *Chem. Soc. Rev.* **2012**, *41*, 2537-2538.
- (21) Xu, X.-D.; Zhao, L.; Qu, Q.; Wang, J.-G.; Shi, H.; Zhao, Y., Imaging-Guided Drug Release from Glutathione-Responsive Supramolecular Porphysome Nanovesicles. *ACS Appl. Mater. Interfaces* **2015**, *7*, 17371-17380.
- (22) Quan, L.; Liu, S.; Sun, T.; Guan, X.; Lin, W.; Xie, Z.; Huang, Y.; Wang, Y.; Jing, X., Near-Infrared Emitting Fluorescent BODIPY Nanovesicles for in Vivo Molecular Imaging and Drug Delivery. *ACS Appl. Mater. Interfaces* **2014**, *6*, 16166-16173.
- (23) Chang, Y.; Yang, K.; Wei, P.; Huang, S.; Pei, Y.; Zhao, W.; Pei, Z., Cationic Vesicles Based on Amphiphilic Pillar 5-arene Capped with Ferrocenium: A Redox-Responsive System for Drug/siRNA Co-Delivery. *Angew. Chem. Int. Ed.* **2014**, *53*, 13126-13130.
- (24) Yao, Y.; Xue, M.; Chen, J.; Zhang, M.; Huang, F., An Amphiphilic Pillar[5]arene: Synthesis, Controllable Self-Assembly in Water, and Application in Calcein Release and TNT Adsorption. *J. Am. Chem. Soc.* **2012**, *134*, 15712-15715.
- (25) Yu, G.; Ma, Y.; Han, C.; Yao, Y.; Tang, G.; Mao, Z.; Gao, C.; Huang, F., A Sugar-Functionalized Amphiphilic Pillar[5]arene: Synthesis, Self-Assembly in Water, and Application in Bacterial Cell Agglutination. *J. Am. Chem. Soc.* **2013**, *135*, 10310-10313.
- (26) Yang, K.; Chang, Y.; Wen, J.; Lu, Y.; Pei, Y.; Cao, S.; Wang, F.; Pei, Z., Supramolecular Vesicles Based on Complex of Trp-Modified Pillar[5]arene and Galactose Derivative for Synergistic and Targeted Drug Delivery. *Chem. Mater.* **2016**, *28*, 1990-1993.
- (27) Shi, B.; Jie, K.; Zhou, Y.; Zhou, J.; Xia, D.; Huang, F., Nanoparticles with Near-Infrared Emission Enhanced by Pillararene-Based Molecular Recognition in Water. *J. Am. Chem. Soc.* **2016**, *138*, 80-83.
- (28) Wang, Y.; Liu, D.; Zheng, Q.; Zhao, Q.; Zhang, H.; Ma, Y.; Fallon, J. K.; Fu, Q.; Haynes, M. T.; Lin, G.; Zhang, R.; Wang, D.; Yang, X.; Zhao, L.; He, Z.; Liu, F., Disulfide Bond Bridge Insertion Turns Hydrophobic Anticancer Prodrugs into Self-Assembled Nanomedicines. *Nano Lett.* **2014**, *14*, 5577-5583.
- (29) Cao, Y.; Li, Y.; Hu, X.-Y.; Zou, X.; Xiong, S.; Lin, C.; Wang, L., Supramolecular Nanoparticles Constructed by DOX-Based Prodrug with Water-Soluble Pillar[6]arene for Self-Catalyzed Rapid Drug Release. *Chem. Mater.* **2015**, *27*, 1110-1119.
- (30) Wang, Y.-X.; Zhang, Y.-M.; Wang, Y.-L.; Liu, Y., Multifunctional Vehicle of Amphiphilic Calix[4]arene Mediated by Liposome. *Chem. Mater.* **2015**, *27*, 2848-2854.
- (31) Vahrmeijer, A. L.; Hutteman, M.; van der Vorst, J. R.; van de Velde, C. J. H.; Frangioni, J. V., Image-guided cancer surgery using near-infrared fluorescence. *Nat. Rev. Clin. Oncol.* **2013**, *10*, 507-518.
- (32) Pansare, V. J.; Hejazi, S.; Faenza, W. J.; Prud'homme, R. K., Review of Long-Wavelength Optical and NIR Imaging Materials: Contrast Agents, Fluorophores, and Multifunctional Nano Carriers. *Chem. Mater.* **2012**, *24*, 812-827.
- (33) Guo, Z.; Zhu, W.; Tian, H., Dicyanomethylene-4H-pyran chromophores for OLED emitters, logic gates and optical chemosensors. *Chem. Commun.* **2012**, *48*, 6073-6084.
- (34) Wu, X.; Sun, X.; Guo, Z.; Tang, J.; Shen, Y.; James, T. D.; Tian, H.; Zhu, W., In Vivo and in Situ Tracking Cancer Chemotherapy by Highly Photostable NIR Fluorescent Theranostic Prodrug. *J. Am. Chem. Soc.* **2014**, *136*, 3579-3588.
- (35) Wang, X.; Ramström, O.; Yan, M., Glyconanomaterials: synthesis, characterization, and ligand presentation. *Adv. Mater.* **2010**, *22*, 1946-53.
- (36) Sutherland, R.; Delia, D.; Schneider, C.; Newman, R.; Kemshead, J.; Greaves, M., Ubiquitous cell-surface glycoprotein on tumor cells is proliferation-associated receptor for transferrin. *Proc. Natl. Acad. Sci. U.S.A.* **1981**, *78*, 4515-4519.
- (37) Zhang, S.; Moussodia, R.-O.; Sun, H.-J.; Leowanawat, P.; Muncan, A.; Nusbaum, C. D.; Chelling, K. M.; Heiney, P. A.; Klein, M. L.; Andre, S.; Roy, R.; Gabius, H.-J.; Percec, V., Mimicking Biological Membranes with Programmable Glycan Ligands Self-Assembled from Amphiphilic Janus Glycodendrimers. *Angew. Chem. Int. Ed.* **2014**, *53*, 10899-10903.

- 1
2
3
4
5
6
7
8
9
10
11
12
13
14
15
16
17
18
19
20
21
22
23
24
25
26
27
28
29
30
31
32
33
34
35
36
37
38
39
40
41
42
43
44
45
46
47
48
49
50
51
52
53
54
55
56
57
58
59
60
- (38) Wu, X.; Lin, B.; Yu, M.; Yang, L.; Han, J.; Han, S., A carbohydrate-grafted nanovesicle with activatable optical and acoustic contrasts for dual modality high performance tumor imaging. *Chem. Sci.* **2015**, *6*, 2002-2009.
- (39) Wu, X.; Yu, M.; Lin, B.; Xing, H.; Han, J.; Han, S., A sialic acid-targeted near-infrared theranostic for signal activation based intraoperative tumor ablation. *Chem. Sci.* **2015**, *6*, 798-803.
- (40) Gorityala, B. K.; Lu, Z.; Leow, M. L.; Ma, J.; Liu, X.-W., Design of a "Turn-Off/Turn-On" Biosensor: Understanding Carbohydrate-Lectin Interactions for Use in Non-covalent Drug Delivery. *J. Am. Chem. Soc.* **2012**, *134*, 15229-15232.
- (41) Sun, W.; Fan, J.; Hu, C.; Cao, J.; Zhang, H.; Xiong, X.; Wang, J.; Cui, S.; Sun, S.; Peng, X., A two-photon fluorescent probe with near-infrared emission for hydrogen sulfide imaging in biosystems. *Chem. Commun.* **2013**, *49*, 3890-3892.
- (42) Jung, D.; Maiti, S.; Lee, J. H.; Lee, J. H.; Kim, J. S., Rational design of biotin-disulfide-coumarin conjugates: a cancer targeted thiol probe and bioimaging. *Chem. Commun.* **2014**, *50*, 3044-3047.
- (43) Wang, C.; Li, Z.; Cao, D.; Zhao, Y.-L.; Gaines, J. W.; Bozdemir, O. A.; Ambrogio, M. W.; Frascioni, M.; Botros, Y. Y.; Zink, J. I.; Stoddart, J. F., Stimulated Release of Size-Selected Cargos in Succession from Mesoporous Silica Nanoparticles. *Angew. Chem. Int. Ed.* **2012**, *51*, 5460-5465.
- (44) Pires, M. M.; Jean, C., Fluorescence imaging of cellular glutathione using a latent rhodamine. *Org. Lett.* **2008**, *10*, 837-840.
- (45) Hou, Y.; Cao, S.; Li, X.; Wang, B.; Pei, Y.; Wang, L.; Pei, Z., One-Step Synthesis of Dual Clickable Nanospheres via Ultrasonic-Assisted Click Polymerization for Biological Applications. *ACS Appl. Mater. Interfaces* **2014**, *6*, 16909-16917.
- (46) Hou, Y.; Cao, S.; Wang, L.; Pei, Y.; Zhang, G.; Zhang, S.; Pei, Z., Morphology-Controlled Dual Clickable Nanoparticles via Ultrasonic-Assisted Click Polymerization. *Polym. Chem.* **2014**, *6*, 223-227.
- (47) Atchutarao, P.; Sureshan, K. M., Reverse-CD mimics with flexible linkages offer adaptable cavity sizes for guest encapsulation. *Chem. Commun.* **2013**, *50*, 317-319.
- (48) Lee, M. H.; Han, J. H.; Kwon, P.-S.; Bhuniya, S.; Kim, J. Y.; Sessler, J. L.; Kang, C.; Kim, J. S., Hepatocyte-Targeting Single Galactose-Appended Naphthalimide: A Tool for Intracellular Thiol Imaging in Vivo. *J. Am. Chem. Soc.* **2012**, *134*, 1316-1322.
- (49) Lv, F.; He, X.; Wu, L.; Liu, T., Lactose substituted zinc phthalocyanine: A near infrared fluorescence imaging probe for liver cancer targeting. *Bioorg. Med. Chem. Lett.* **2013**, *23*, 1878-1882.
- (50) Mou, Q.; Ma, Y.; Zhu, X.; Yan, D., A small molecule nanodrug consisting of amphiphilic targeting ligand-chemotherapy drug conjugate for targeted cancer therapy. *J. Control. Release* **2016**, *230*, 34-44.

For Table of Contents Only

